THEORETICAL AND EXPERIMENTAL STUDY FOR NEW TITANIUM METAL COMPLEXES IN BIOPHYSICAL APPLICATIONS

Ali S. Hasan[a,*], Mohammed A. Akraa[a], Salim J. Abbas[b]

[a] University of Babylon, College of Materials Engineering, Hilla, Iraq
E-mail*:alisalahphy@yahoo.com
E-mail:dmamah73@gmail.com
[b] Al-Furat Al-wsat Technical University, Babylon Technical Institute, Hilla, Iraq
E-mail: salimj70@gmail.com

Abstract

In this research, new titanium metal complexes were designed and prepared for use in biophysical applications, because titanium is biocompatible (non-toxic and accepted by the body). New models of TiMC were designed and prepared by DFT/B3LYP method with SDD base sets and chemical vapor deposition technology, respectively. Structural, electronic transitions, and surface morphology properties were calculated by Gaussian 09 program package, XRD and SEM. The optimized structures for molecules under study have been found in great concurrence with empirical information. The results showed that these complexes have an electronic transition, UV-Vis spectrum, low band gaps, low chemical potential and are softer, can easily interact with enzymes because the enzymes are big soft molecules. The present study is aimed at investigating the effect of TiMC in Biophysics. Moreover, we used an orbital analysis, counting the 3-D electron density and electrostatic potential surfaces to find out the possible orbital hybridization for molecules, thus determining the biological effectiveness of the molecules under study.

Keywords: Titanium, electronic transitions and surface morphology properties, DFT, Biophysical applications

摘要

在这项研究中，由于钛具有生物相容性（无毒且被人体接受），因此设计并制备了用于生物物理应用的新型钛金属配合物。采用 DFT / B3LYP 方法，SDD 基组和化学气相沉积技术分别设计和制备了 TiMC 的新模型。通过高斯 09 程序包，XRD 和 SEM 计算结构，电子跃迁和表面形态特性。已发现与实验信息非常吻合的是，正在研究的分子的优化结构。结果表明，这些复合物具有电子跃迁，UV-Vis 光谱，低带隙，低化学势且较软，因为这些酶是大的软分子，因此很容易与酶相互作用。本研究旨在研究 TiMC 在生物物理学中的作用。此外，我们使用了轨道分析，对 3-D 电子密度和静电势表面进行了计数，以找出分子的可能轨道杂交，从而确定了所研究分子的生物学有效性。

关键词: 钛，电子跃迁和表面形态特性，**DFT**，生物物理应用

I. INTRODUCTION

There is no exaggeration to say that radiation therapy is the most important and effective tool to treat the cancer cell. The conventional radiotherapy is applied to treat half the total number of cancer tumors worldwide. However, photons interact with all the tissues of their track before reaching their target. This action creates damage to much of normal cells and subsequently, may cause secondary cancers [1]. Based on the above, there should be another

alternative way of treatment. Thus, the so-called particle therapy was found, i.e., radiotherapy with charged external particle beams for cancer treatment [1], [2]. This new kind of therapy is superior to x-ray, whereas, it is based on tumors enrichment with elevated Z-compounds. As a contemporary strategy it aims to raise the irradiation influences through the intensification of essential (electronic) forms [1], [3].

The verification of the rule of this methodology was first exhibited with platinum complexes (chloroterpyridine platinum, PtTC) utilized as radio-enhancers. It is found that the nanosize bio-harm is the most deadly to living cells, the enhancement of these sorts of damage is a noteworthy test of the procedure [4], [5]. The assortment and degree of metal particle inclusion have been as evaluated recently. However, they have an extremely long history in toxicology, prescription, and pharmacology. For example, Mo, Co, Mn, Ni, Cu, V, Zn, Fe and Cr among the progress metals are exceptionally fundamental to life. The uncommon earth metals likewise are involved in the natural action [6], [7]. Some different components like Ag, Os, Pd, Ir, Ti, Au, Pt, and others have some restorative worth an account of their utilization in treatment. The physiological action could conceivably be related straightforwardly to the existence of complex particles and their fixation and this reality raises another issue. However, the science of metal particles is influenced by the dissolution or assimilation of the metal particles on the surface [7]-[9].

This paper presents new metallic complexes of a central Titanium atom bonded to different ligands (tetrafluoride, di-fluoride di-pyridine, and di-fluoride di-pyrimidine). The search comprises many unique features of these proposed complexes as its crystallinity, low band gap, low chemical potential, and high ability to interact with enzymes.

II. METHODS/MATERIALS
A. Computational Method

GaussView 5.0.8 program [10] was used to draw the initial structure of the complex and provide the database for it is the input file. The calculations were executed by using Gaussian 09 package of programs [11]. Titanium metal complexes (TiMC) were fully relaxed by employing B3LYP-SDD/DFT in the gas phase. The B3LYP combination of exchange and correlation functional in DFT is applied to all calculations of the electronic structure. The electronic excitation energy was calculated for the relaxed metal complex by employing the

B3LYP/DFT method with SDD basis sets. The B3LYP-SDD/DFT method has been verified to be reliable for calculating spectra properties of many transition metal complexes.

B. Preparation of Titanium Metal Complexes

The chemical vapor deposition (CVD) is a coating technology involving deposition of a solid material from a gaseous phase on a heated substrate to form a desired thin film [12]. The deposit can be framed by a response between the vapor and the same substrate. Multicomponent tough coatings (TiMC) were deposited on a glass substrate. The TiMC coatings doped with (di-pyridine and di-pyrimidine) were saved at various precipitation temperatures ranging from 450°C to 750°C, and under similar fluorine flow rates. A gas-phase deposition process technique CVD is shown in Figure 1. A gas-phase deposition technique was employed here as a new tool for the hard film deposition. The unit of powder dissipation used in this work comprises a vacuum tube heater of high-temperature type GSL-1600-60X. The latter was utilized to provide the metal gases for the sedimentary procedure. All the requested gases were supplied into the chambers equipped with a controlled system of gas transmission. This supply consists of two feeding lines viz: Ti-Base vapor and fluoride gas. At that point in the sedimentation chamber which is the reactor to sediment Ti-Base coatings a perfect face film is obtained. The relieving process of the non-responded chemical substances can be achieved through the exhausting instrument of gas.

Figure 1. Coating arrangement equipment used in this study: 1. Evaporation part, 2. Ti-Based vapor path, 3. Sedimentation Chamber, 4. Quartz sedimentation pipe, 5. Exhaust gas part, 6. Thermometer.

III. RESULTS AND DISCUSSION

The relaxed structure of TiMC in Figure 2 was optimized at the minima by utilizing the hybrid functional B3LYP-DFT with SDD basis sets. The calculated values of the optimal parameters for the complex are listed in Table 1.

Table 1.
The optimal parameters for the complexes.

Bond	Value (nm)	Angle	Value (deg.)
Ti-F	18.50-19.00	Ti-F-Ti	90
Ti-C	20.90-21.00	Ti-F-C	90
C-C	13.93-14.20	C-C-C	118.505
C-N	13.47-13.68	C-N-C	117.210
C-H	11.04-11.09	N-C-H	115.720

A- Titanium Tetrafluoride metal complex

B- Titanium di-fluoride di-pyridine metal complex

C- Titanium di-fluoride di-pyrimidine metal
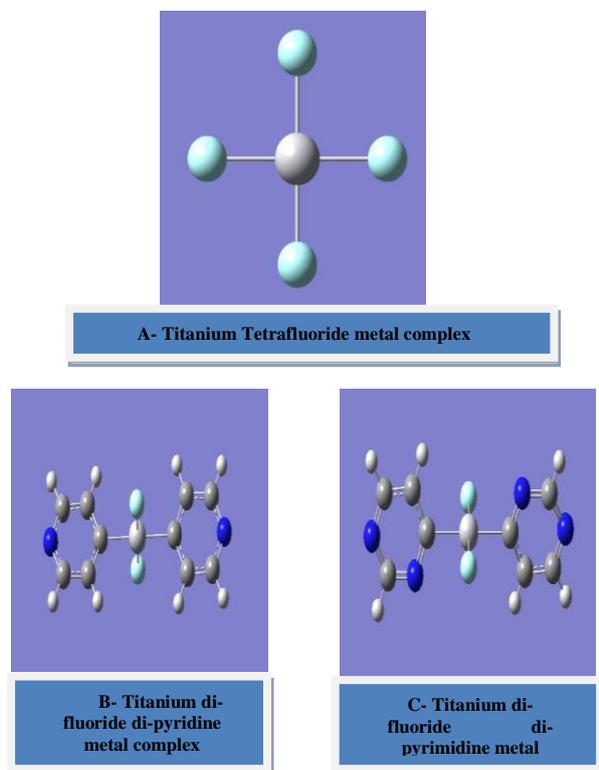
Figure 2. The optimized structure of TiMC.

The above outcomes demonstrated that the hybrid functional DFT-B3LYP with SDD basis sets is effective to evaluate the enhanced structure of TiMC. The advanced structure of the TiMC has been found in a decent concurrence with the trial information.

Table 2 announces the results of the total energy ET in a.u and the virial ratio (-V/T), and some computed energies in eV of TiMC, calculated depending on Koopman's theorem. These calculations are carried out by implementing a B3LYP/6-31G level of DFT and included the ionization energy IE, electron affinity EA, electronegativity X, electrochemical hardness H, electronic softness S and electrophilic index W. To estimate the reactivity and the stability of the complexes, B3LYP-SDD/DFT -based descriptors were calculated:

$$\mu = \left(\frac{\partial E}{\partial N}\right)_{V(\vec{r}),T} \tag{1}$$

$$\eta = \frac{1}{2}\left(\frac{\partial^2 E}{\partial N^2}\right)_{V(\vec{r}),T} \tag{2}$$

$$S = \frac{1}{2\eta} \tag{3}$$

$$\boxed{H} = \frac{\mu^2}{2\eta} \tag{4}$$

$$\chi = \frac{(IP + EA)}{2} \tag{5}$$

$$\eta = \frac{(IP - EA)}{2} \tag{6}$$

Then, using Koopman's theorem the above equations can be given as [7]:

$$\chi = \frac{(E_{HOMO} + E_{LUMO})}{2} \tag{7}$$

$$\eta = \frac{(E_{HOMO} - E_{LUMO})}{2} \tag{8}$$

Table 2.
The calculated energies of TiMC.

Molecule	Titanium Tetrafluoride metal complex	Titanium di-fluoride di-pyridine metal complex	Titanium di-fluoride di-pyrimidine metal complex
ET (a.u)	-457.995	-753.490	-785.552
HOMO(eV)	-0.4077	-0.2364	-0.2260
LUMO (eV)	-0.2428	-0.1398	-0.1343
E_g(eV)	0.165	0.097	0.092
-V/T	2.0863	2.0077	2.0522
IE(eV)	0.408	0.236	0.226
EA(eV)	0.243	0.140	0.134
X(eV)	0.325	0.188	0.180
H(eV)	0.082	0.048	0.046
W(eV)	0.642	0.366	0.354
S(eV)$^{-1}$	6.066	10.343	10.915

Table 2 shows that the total energy of Titanium Tetrafluoride is less than the energy of Titanium di-fluoride di-pyridine and Titanium-di-fluoride di-pyrimidine. With the addition of the complex, the total energy increases due to the current decrease in the electronegativity and this confirms the change in (-V/T). We also note the increase in the electronic flexibility of the complex and this is very important in the mechanism of dealing with medical and vitality applications, corresponding to the increase in its possession, so that it has a sudden automatic endurance, an indication of the acquisition ability and electronic loss [6], [13].

Figure 3 and Figure 4 show the 3-D electron density (TD) and electrostatic potential (ESP) surfaces of TiMC obtained from the B3LYP/SDD level of theory.

As shown in Figure 4, the distribution of ESP for titanium complex results from the strength of repulsion or attraction of the surrounding region of each molecule. In other words, the distribution of ESP varies according to the sub-sub-groups, ESP of the surface is stable and balanced for the Titanium Tetrafluoride complex due to the high

compatibility and balance in addition to the sides, but it changes completely with the other complexities due to the difference in the number of atoms and electrons so that every effort tries to maintain regularity and therefore begins to crawl negative charges. The ESP surfaces for these compounds showed the potentials were dragged toward the areas of high electronegativity, and therefore, give one to understand in determining the effective end positions of each compound in connection with the surrounding species or molecules to construct new metal complexes [7], [14].

We observe from Figure 3 that with the addition of Titanium di-fluoride-di-pyridine metal complex the surface is compressed in a 90° angle towards negative charges. While adding Titanium di-fluoride-di-pyrimidine metal complex the surface is rounded and collected irregularly because it wants to converge on the self to scale the corresponding form due to the greater electronegativity of pyrimidine [13].

A- Titanium Tetrafluoride metal complex

B- Titanium di-fluoride di-pyridine metal complex

C- Titanium di-fluoride di-pyrimidine metal complex
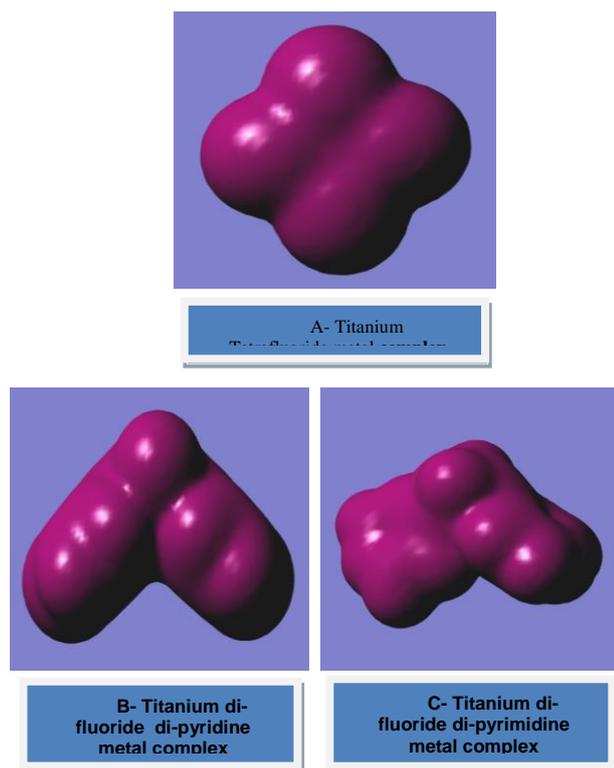
Figure 3. The 3-D electron density TD surfaces of TiMC.

Thus, we can deduce ESP and TD, the symmetry found in images of HOMO and LUMO levels of the complex and as in Figure 5 so that the control of negative charges is more than positive charges and how to form single and double bonds.

Figure 6 shows the same behavior for all complexes with a wavelength of 220-400 nm but

according to the intensity of each complex. This confirms a slight decrease in the energy gap of the complexes (di-pyridine and di-pyrimidine) as a result of the convergence of (HOMO) and (LUMO) levels with each other [13], [15].

A- Titanium Tetrafluoride metal complex

B- Titanium di-fluoride di-pyridine metal complex

C- Titanium di-fluoride di-pyrimidine metal complex
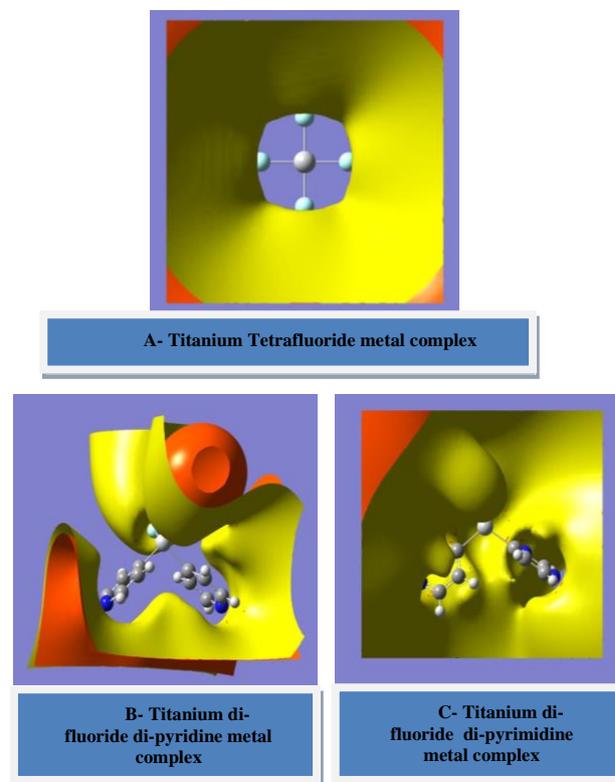
Figure 4. The electrostatic potential ESP surfaces of TiMC.

The X-ray diffraction pattern of the TiMC is shown in Figure 7 and the peak details are given in Table 3 which reports that the absence of spurious diffractions indicates crystallographic purity. The 2θ at peak (25.7099°, 28.6285° and 40.1258°) confirms the Ti anatase structure. Strong diffraction peaks at (25.7099°, 48.4267°), (28.6285°, 51.3975°) and (32.5896°, 56.3478°) indicate Titanium metal in the anatase phase respectively for the complexes. There is no pseudo diffraction peak found in the complexes. The high 2θ peaks confirm its anatase structure.

Table 3.
XRD Data of TiMC

Species	2 Theta	d (nm)	FWHM (deg)	Intensity (Counts)
A- Titanium Tetrafluoride metal complex	25.7099	34.6228	0.50150	8025
	48.4267	18.7816	0.47170	1692
	38.1893	23.5472	0.49860	1192
B-Titanium di-fluoride	28.6285	34.9436	0.47730	5289
	51.3975	18.8580	0.45800	1507

di-pyridine metal complex	40.1258	23.6763	0.48030	1127
C-Titanium di-fluoride di-pyrimidine metal complex	32.5896	34.9436	0.47624	4687
	56.3478	18.7816	0.47258	1098
	45.36987	23.5472	0.49651	4458

HOMO · A- Titanium Tetrafluoride metal complex · LUMO

HOMO · B- Titanium di-fluoride di-pyridine metal complex · LUMO

HOMO · C- Titanium di-fluoride di-pyrimidine metal complex · LUMO
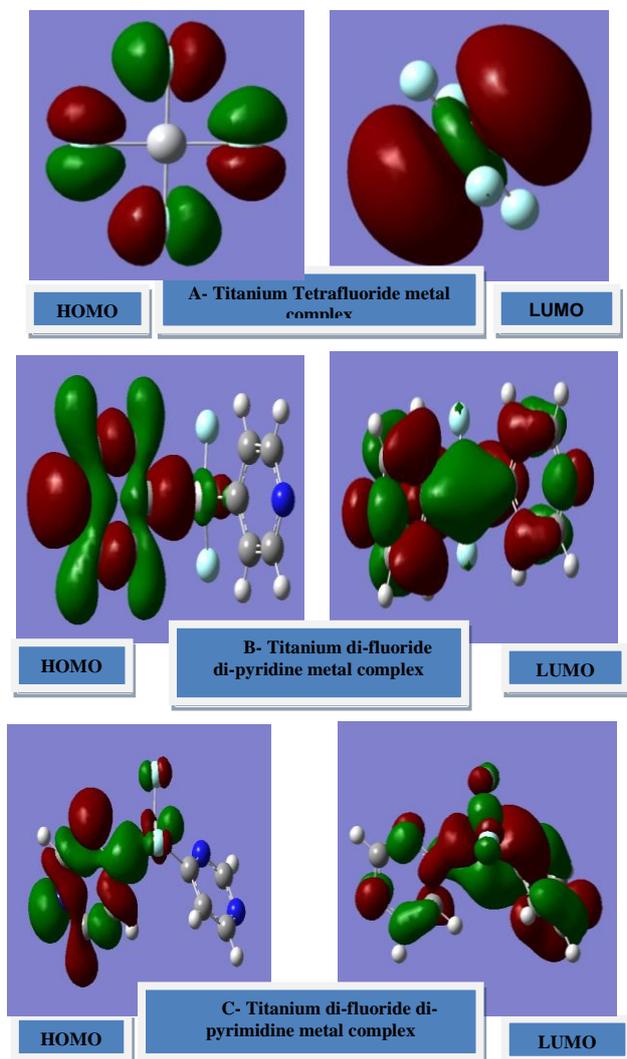
Figure 5. The 3-D distribution of HOMO and LUMO of TiMC.

A- Titanium Tetrafluoride metal complex

B- Titanium di-fluoride di-pyridine metal complex

C- Titanium di-fluoride di-pyrimidine metal complex
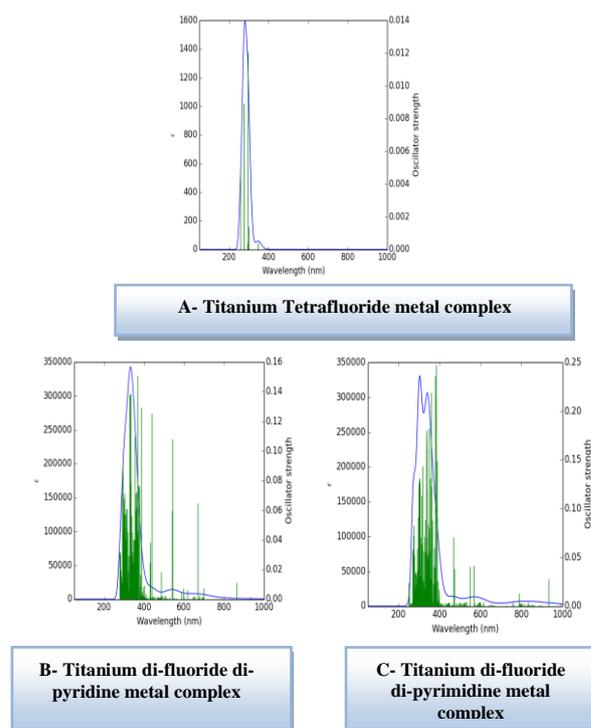
Figure 6. The UV-VIS Spectrum of TiMC.

Titanium Tetrafluoride metal complex

Titanium di-fluoride di-pyridine metal complex
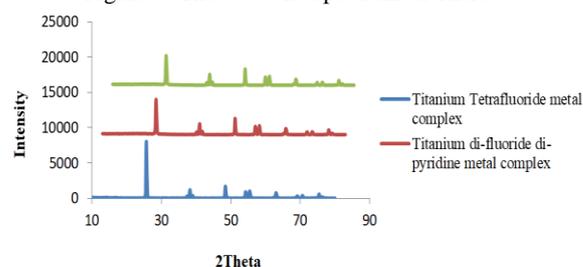
Figure 7. XRD pattern of TiMC.

The intensity of XRD peaks of the complexes reflects that the created nanoparticles are crystalline and broad diffraction peaks indicate very small size crystallite [12], [13].

Figure 8 illustrates that coating is continuous and uniform. The Titanium layer is deposited throughout the surface in a globular form. At higher enlargement (50, 100, 200 nm), many pores can be seen and the grain diameters are found to be 10-20 nm. All SEM photos show that the acquired surfaces are porous. The cracks in the surface layer are visible beyond the pores, which may be symptomatic of too rapid growth in the volume of the layer. It is worth mentioning that the increase in the di-pyridine and di-pyrimidine amount does not result in such cracks [12], [15].
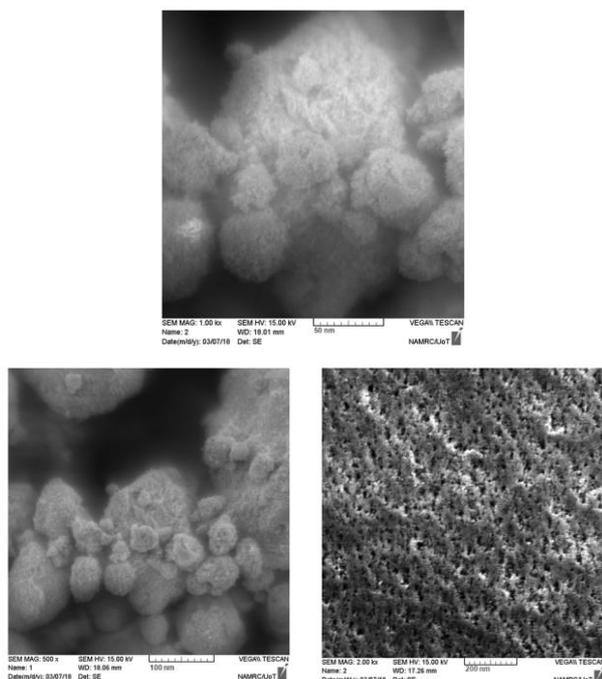
Figure 8. SEM images of TiMC by CVD.

IV. CONCLUSION

B3LYP-SDD/DFT calculations were used to study the activity of some suggested Titanium Metal Complexes according to the coordination of these complexes. The results showed the bonds of the Ti agree with those obtained from the empirical data. Frontier orbitals (EHOMO and ELUMO), energy gap, global hardness and softness were calculated to predict the activity of the complex. The results of the quantum chemical parameters showed that the Titanium Tetrafluoride metal complex has a small energy gap with high activity to interact with other surrounding species. It has been observed that coating is continuous and uniform. The Titanium layer is deposited throughout the surface in a globular form. At higher enlargement (50, 100, 200 nm), many pores can be seen and the grain diameters are found to be 10-20 nm. The intensity of XRD peaks of the complexes reflects that the created nanoparticles are crystalline and broad diffraction peaks indicate very small size crystallite.

REFERENCES

[1] LACOMBE, S., PORCEL, E. and SCIFONI, E. (2017) Particle therapy and nanomedicine: state of art and research perspectives. *Cancer Nanotechnology*, 8(1), pp. 1-17, doi: 10.1186/s12645-017-0029-x.

[2] ELLAHIOUI, Y., PRASHAR, S. and GÓMEZ-RUIZ, S. (2017) Anticancer applications and recent investigations of metallodrugs based on gallium, tin and titanium. *Inorganics,* 5(1), pp. 4-27, doi: 10.3390/inorganics5010004.

[3] KONG, L., GAO, J., HU, J. et al. (2016) Phase I/II trial evaluating concurrent carbon-ion radiotherapy plus chemotherapy for salvage treatment of locally recurrent nasopharyngeal carcinoma. *Chinese Journal of Cancer*, 35(1), pp. 101-112, doi: 10.1186/s40880-016-0164-5.

[4] GERMAN, R.M. (2013) Progress in titanium metal powder injection molding. *Materials*, 6(8), pp. 3641–3662, doi: 10.3390/ma6083641.

[5] TSHUVA, E.Y. and MILLER, M. (2018) Coordination complexes of titanium (IV) for anticancer therapy. A chapter in *Metallo-Drugs: Development and Action of Anticancer Agents.* doi: 10.1515/9783110470734-008.

[6] PING, T., TANG, X.-Y., LI, B.-X., LIU, J.-Y., and LI, Y.-S. (2012) Synthesis and characterization of novel titanium complexes bearing [ONX]-type β-enaminoketonato ligands and their application to ethylene (co)polymerization. *Dalton Transactions*, 41, pp. 7390-7398, doi: 10.1039/c2dt30326d.

[7] CASTRO, M., LIU, S.-R., ZHAI, H.-J., WANG, L.-S., and WILEY, W. (2003) Structural and electronic properties of small titanium clusters: A density functional theory and anion photoelectron spectroscopy study. *Journal of Chemical Physics,* 118(5), pp. 2116–2123. doi: 10.1063/1.1532000.

[8] KOSTOVA, I. (2012) Titanium and Vanadium Complexes as Anticancer Agents. *Anti-Cancer Agents in Medicinal Chemistry*, 9(8), pp. 827-842, doi: 10.2174/187152009789124646.

[9] ASSI, H., MOUCHAHAM, G., STEUNOU, N., DEVIC, T., and SERRE, C. (2017) Titanium coordination compounds: From discrete metal complexes to metal-

organic frameworks. *Chemical Society Reviews*, 46, pp. 3431-3452. doi: 10.1039/c7cs00001d.

[10] Dennington, R., Keith, T., & Millam, J. (2009). GaussView (Version 5): Semichem Inc., Shawnee Mission.

[11] FRISCH, M.J., TRUCKS, G.W., SCHLEGEL, H.B., SCUSERIA, G.E., ROBB, M.A., CHEESEMAN, J.R., FOX, D.J. (2009) *Gaussian 09, Revision E.01.* Wallingford, CT.

[12] SHIRAISHI, N., ISHIKO-UZUKA, R., TAKAHASHI, K., OGAWA, T., ANADA, T. et al. (2019) Effect of functionally-Graded Calcium titanate film, prepared by metal-organic chemical vapor deposition, on titanium implant. *Applied Sciences (Switzerland)*, 9, 172, pp. 1-11, doi: 10.3390/app9010172.

[13] SHAYESTEH, P., TSYSHEVSKY, R., URPELAINEN, S., ROCHET, F., BOURNEL, F., et al. (2019) 'Experimental and theoretical gas phase electronic structure study of tetrakis (dimethylamino) complexes of Ti(IV) and Hf(IV)', *Journal of Electron Spectroscopy and Related Phenomena*, 234, PP. 80-85, doi: 10.1016/j.elspec.2019.05.016.

[14] MOROZOV, A.G., FEDUSHKIN, I.L., IRRAN, E., and GROHMANN, A. (2018) Titanium(IV) complexes supported by a dianionic acenaphthenediimine ligand: X-ray and spectroscopic studies of the metal coordination sphere. *Inorganic Chemistry Communications*, 95, PP. 50-55, doi: 10.1016/j.inoche.2018.07.006.

[15] SURLEVA, A., ATANASOVA, P., KOLUSHEVA, T., and COSTADINNOVA, L. (2014) Study of the complex equilibrium between titanium (IV) and tannic acid. *Journal of Chemical Technology and Metallurgy*, 49(6), pp. 594–600.

参考文:

[1] LACOMBE，S.，PORCEL，E.和 SCIFONI，E.（2017）粒子疗法和纳米医学：最新技术和研究观点。癌症纳米技术，8（1），第 1-17 页，doi：10.1186/s12645-017-0029-x。

[2] ELLAHIOUI，Y.，PRASHAR，S.和 GÓMEZ-RUIZ，S.（2017）抗癌应用和基于镓，锡和钛的金属药物的最新研究。无机物，5（1），第 4-27 页，doi：10.3390/inorganics5010004。

[3] KONG，L.，GAO，J.，HU，J.等。（2016）I／II 期试验评估并发碳离子放疗加化疗对局部复发性鼻咽癌的挽救治疗。中华癌症杂志，35（1），第 101-112 页，doi：10.1186/s40880-016-0164-5。

[4] GERMAN，R.M.（2013）钛金属粉末注射成型的进展。材料，6（8），第 3641–3662 页，doi：10.3390/ma6083641。

[5] TSHUVA，E.Y。和 MILLER，M.（2018）钛（IV）的配合物用于抗癌治疗。金属药物：抗癌药的发展和作用中的一章。doi：10.1515 / 9783110470734-008。

[6] PING，T.，TANG，X.-Y.，LI，B.-X.，LIU，J.-Y.，和 LI，Y.-S.（2012）带有 [ONX]型 β-烯氨基酮配体的新型钛配合物的合成与表征及其在乙烯（共）聚合中的应用。道尔顿交易，41，第 7390-7398 页，doi：10.1039/c2dt30326d。

[7] CASTRO，M.，LIU，S.-R.，ZHAI，H.-J.，WANG，L.-S。和 WILEY，W.（2003）小型钛簇的结构和电子性能：A 密度泛函理论和阴离子光电子能谱研究。化学物理学杂志，118（5），第 2116-2123 页。 doi：10.1063/1.1532000。

[8] KOSTOVA，I。（2012）作为抗癌剂的钛和钒配合物。药物化学中的抗癌药，9（8），第 827-842 页，doi：10.2174/187152009789124646。

[9] ASSI，H.，MOUCHAHAM，G.，STEUNOU，N.，DEVIC，T.和 SERRE，C.（2017）钛配位化合物：从离散的金属络合物到金属有机骨架。化学学会评论，46，第 3431-3452 页。 doi：10.1039/c7cs00001d。

[10] DENNINGTON，R.，KEITH，T.，和 MILLAM，J.（2009）。高斯视图（版本 5）：Semichem Inc.，Shawnee Mission。

[11] FRISCH，M.J.，TRUCKS，G.W.，SCHLEGEL，H.B.，SCUSERIA，G.E.，ROBB，M.A.，CHEESEMAN，J.R.，FOX，D.J.。（2009）高斯 09，修订版 E.01。康涅狄格沃灵福德。

[12] SHIRAISHI, N., ISHIKO-UZUKA, R., TAKAHASHI, K., OGAWA, T., ANADA, T.

等。（2019）通过金属有机化学气相沉积制备的功能梯度钛酸钙膜对钛植入物的影响，应用科学（瑞士），9，172，第 1-11 页，doi：10.3390/app9010172。

[13] SHAYESTEH，P.，TSYSHEVSKY，R.，URPELAINEN，S.，ROCHET，F.，BOURNEL，F.等。（2019）"Ti（IV）和 Hf（IV）的四（二甲基氨基）配合物的实验和理论气相电子结构研究"，《电子光谱学和相关现象》，234，第 80-85 页，doi：10.1016/j.elspec.2019.05.016。

[14] MOROZOV，A.G.，FEDUSHKIN，I.L.，IRRAN，E. 和 GROHMANN，A.（2018）钛（IV）配合物由双阴离子啶二胺配体支持：金属配位球的 X 射线和光谱研究。无机化学通讯，95，第 50-55 页，doi：10.1016/j.inoche.2018.07.006。

[15] SURLEVA，A.，ATAANASOVA，P.，KOLUSHEVA，T。和 COSTADINNOVA，L。（2014），研究了钛（IV）和鞣酸之间的复杂平衡。化学技术和冶金学报，49（6），第 594–600 页。